

## ARTICLE

# Effects of Non-specific and Specific Solvation on Adsorption of BPTI on Au Surface: Insight from Molecular Dynamics Simulation

Wei Yang, Li-yun Zhang, Meng-long Li, Xue-mei Pu\*, Nan-rong Zhao\*

Faculty of Chemistry, Sichuan University, Chengdu 610064, China

(Dated: Received on May 15, 2013; Accepted on May 23, 2013)

Proteins adsorption at solid surfaces are of paramount important for many natural processes. However, the role of specific water in influencing the adsorption process has not been well understood. We used molecular dynamics simulation to study the adsorption of BPTI on Au surface in three water environments (dielectric constant model, partial and full solvation models). The result shows that a fast and strong adsorption can occur in the dielectric environment, which leads to significant structure changes, as confirmed by great deviation from the crystal structure, largely spreading along the Au surface, rapid lose in all secondary structures and the great number of atoms in contact with the surface. Compared to the dielectric model, slower adsorption and fewer changes in the calculated properties above are observed in the partial solvation system since the specific water layer weakens the adsorption effects. However, in the partial solvation system, the adsorption of polar Au surface causes a significant decrease in the specific hydration around the protein, which still results in large structure changes similar to the dielectric system, but with much less adsorption extent. Enough water molecules in the full solvation system could allow the protein to rotate, and to large extent preserve the protein native structure, thus leading to the slowest and weakest adsorption. On the whole, the effects of non-specific and specific solvation on the protein structure and adsorption dynamics are significantly different, highlighting the importance of the specific water molecule in the protein adsorption.

**Key words:** Adsorption, Au surface, Implicit water, Partial solvation, Full solvation

## I. INTRODUCTION

Protein adsorption at solid surfaces has attracted considerable research interests from experiments and theories [1–6]. These interests are inspired by its application in various areas, including biosensor, nano electric functional devices, biological functional materials medicine, pharmaceutical sciences, and so on [7–11]. Advances of our knowledge of protein adsorption are mainly achieved through experimental approaches. However, there are still widely different and even contradictive opinions how to explain structural rearrangements and adsorption dynamics associated with functional changes, despite considerable progress in this field [12]. The reason is mainly due to the complexity of the system composition and the structure of protein so that it is difficult for experiment to detect subtle conformational changes of protein upon adsorption and detailed dynamics behaviors. Thus, the adsorption mechanism of proteins on solid surfaces is still not fully understood, especially at a molecular level, which limits its further application [12–14].

Molecular dynamics simulations could provide a molecular level view of the intermolecular interaction and can reveal dynamic behavior of proteins [15–18]. Thus, the method has been successfully used to study the adsorption of protein on the surfaces [4–22]. The surfaces or sorbents in the previous researches include graphite [19–22], SiO<sub>2</sub> [23–25], TiO<sub>2</sub> [26–28], MgO [29], Au [30–32], Pd or Au/Pd [33], Mg<sub>3</sub>Si<sub>2</sub>O<sub>5</sub>(OH)<sub>4</sub> [34], and Ca<sub>10</sub>(PO<sub>4</sub>)<sub>6</sub>(OH)<sub>2</sub> [35], etc. The systems studied range from peptides to various kinds of proteins, for example, bovine pancreatic trypsin inhibitor (BPTI) [29], hen egg white lysozyme (HEWL) [23–25], human serum albumin (HSA) [19, 34], bovine serum albumin (BSA) [21], bone morphogenetic protein-2 (BMP-2) [22, 27], fibrinogen (FIB) [26, 28], etc. These researches mainly concerned the protein's conformational changes and some special properties of adsorption. For example, Raffaini and Ganazzoli investigated the adsorption of HSA and Lysozyme proteins on the hydrophobic surface of graphite in 2003 and 2009, respectively, using an effective dielectric medium to describe the aqueous environment [19, 20]. In 2012, they utilized the same method to simulate the albumin subdomain and the fibronectin type I adsorption on the titanium dioxide polymorphs [28]. The results showed that it was easy for the proteins to produce conformational changes

\*Authors to whom correspondence should be addressed. E-mail:  
xmpuscu@scu.edu.cn, zhaonanr@scu.edu.cn

in the implicit water environment and all secondary structure of proteins almost disappeared in the final phase of adsorption. Mücksch and Urbassek studied the adsorption of BSA on graphite in the implicit water environment and found that the adsorption more or less completely destroyed the lower part of the protein bonded to graphite [21]. The adsorption of HSA protein on chrysotile surface ( $Mg_3Si_2O_5(OH)_4$ ) was studied using molecular dynamics (MD) method and an effective distance-dependent dielectric constant to model aqueous environment, which displayed a very large spreading of the protein on the surface, almost a single monolayer [34]. Another study on the adsorption of a fibronectin type III module on rutile (110) surface in vacuum was carried out [26], suggesting that the simulation in vacuum environment is similar to those in a dielectric constant due to large deformations of protein also observed in the final of simulation. As shown above, the implicit water model was frequently used in the MD studies on the protein adsorption since it was suggested to be an efficient way to speed up the adsorption of protein to surface.

On the other hand, some MD researches mainly used explicit water model to investigate the adsorption of protein. For example, Goldstein studied the adsorption of BPTI to MgO surface [29]. Mulheran investigated the charged solid surface to adsorb the HEWL [23–25]. Gottschalk *et al.* [31], Maranas *et al.* [30, 32], and Heinz *et al.* [33] discussed the adsorption of some peptides on Au surface. The hydroxyapatite ( $Ca_{10}(PO_4)_6(OH)_2$ ) was investigated as sorbent to explore the adsorption and desorption of the fibronectin on it [35]. Interestingly, Mroginski *et al.* used MD method to study the adsorption of BMP-2 to hydrophobic graphite and hydrophilic titanium dioxide rutile in explicit water environment [27] and found that their results were opposite to the observations derived from Mücksch and Urbassek [22], who examined the adsorption of BMP-2 on graphite using an implicit aqueous environment. Thus, they suggested that an implicit model of the solvent may be inadequate to describe the adsorption of BMP-2. In addition, Maranas *et al.* investigated peptide adsorption on the gold surface in three circumstances [30]: peptides in solution without the gold surface, solvated peptides approaching to a gold surface, and peptides approaching a gold surface in vacuum. A comparison of these results also indicated that the water could form H-bond with the titanium dioxide surface and mediate interaction between the surface and the protein, showing the important effect of the explicit water on the adsorption of protein. Furthermore, they suggested that more and further studies should be needed to address the effect of the specific water. Recently, Corni *et al.* used first-principles simulation to study the adsorption of  $\beta$ -sheet polyserine peptide on Au surface in the explicit water and indicated that there is charge density spreading between interstitial water molecules and the Au surface, which contributes

to protein-gold surface recognition [36].

As mentioned above, the implicit and explicit water were two main environment models for the MD studies in the field and their results provided valuable information at the molecular level for clarifying the adsorption mechanism, effectively supplementing the experimental investigations. However, it is also noted that there are some difference [37–40], even contradictive results derived from MD studied using the two water models, which disfavor our understanding on the adsorption mechanism. As accepted, the dielectric constant used in implicit solvent model could account for large part of the solvent effect. But, the model neglects any reference to the atomistic nature of the solvent. Thereby, the solvent effect derived from the implicit model indicates non-specific electrostatic effects (non-specific solvation), not considering any specific solute-solvent interactions, for example, hydrogen bonding. However, it was known that water, especially water molecules bound to the protein, plays an important role in the structural, functional, and dynamical properties of proteins through forming a variety of specific hydrogen bonds with the C=O and N–H groups of the peptide unit [41, 42].

Some previous MD works on peptide and protein adsorption also mentioned the importance of explicit water, mainly on basis of a comparison of the result in explicit water with one in vacuum [30, 36]. But, no further and detailed MD works were carried out to address the difference between the specific solvation derived from explicit water model and non-specific solvation derived from implicit water one. The information is important to clarify the role of specific interaction of protein-water-surface in influencing adsorption, which is one key to understand the mechanism of adsorption. In fact, some contradictive results between the two water models should stem from the difference in the effects of non-specific and specific solvation on the protein adsorption.

Based on the consideration above, we, in the work, chose bovine pancreatic trypsin inhibitor (BPTI) as a protein model, which was investigated on the MgO surface [29], and designed three aqueous environments to study its adsorption on gold surface. One water environment is to use dielectric constant of water (implicit water model). The second is to use a 2.5 Å layer of explicit water to solvate the protein and the gold surfaces since the water layer is generally considered as the first hydration shell of protein [43] and surface [33]. The water molecules in the layer are considered to be in contact with the protein and to play more important roles in the protein structure and function relative to bulk water. In the third water environment, the protein and the gold surface are fully solvated with the explicit water. By comparison of these systems, we could gain direct insight into the effects of non-specific and specific solvation on the protein adsorption. In addition, the result derived from the partial solvation system could help us to understand the role of bound water in the protein

adsorption. Our objective is to shed light on the effect of specific water, accordingly providing useful information at the molecular level for better understanding the adsorption mechanism.

## II. SIMULATION METHODS

All the simulations were performed using Visualizers and Discover modules implemented in Accelry's Materials Studio 4.2. The consistent valence force field (CVFF) [33, 44] extended for accurate Lennard-Jones parameters for fcc metals (Ag, Al, Au, Cu, Ni, Pb, Pd, Pt) [33, 44] was employed for the protein and the Au surface. The explicit water was represented by the TIP3P model [45, 46].

The X-ray structure of BPTI protein was obtained from the Protein Data Bank (the PDB entry code is 6pti), which contains 57 amino acids and 73 crystallographic water molecules. We added hydrogen atoms in the calculation position of protein and corresponded the overall protonation state to pH=7.0, resulting in a total of charge +4e. Four chloride ions were introduced near positively charged groups as counter ions to maintain charge neutrality.

The Au(111) surface was generated from the Materials Studio database by cleaving surface (111) and periodically repeating the crystal cell along the two axis ( $x, y$ ), then a five-layer with  $69.2 \text{ \AA} \times 59.9 \text{ \AA}$  in the  $x, y$  direction was constructed as the Au surface in the simulation.

Three types of water environments were considered in the work. One is to use a distance-dependent dielectric constant of water ( $\varepsilon_r=78.3$ ) [20] to model aqueous solution (labeled as A system or dielectric system), as shown in Fig.1A. The second is to use two 2.5 Å explicit water layers around the protein and the surface (water density is  $1.0 \text{ g/cm}^3$ ), respectively (labeled as B system or partial solvation system, see Fig.1B). The third is to fully solvate the protein and the surface with 5000 water molecules at a density of  $1.0 \text{ g/cm}^3$  (labeled as C system or full solvation system), as shown in Fig.1C. Box dimensions were typically  $69.2 \text{ \AA} \times 59.9 \text{ \AA} \times z$  whereby the adjusting box height  $z$  amounts to about 130 Å after adding enough vacuum layer up to 80 Å on the upside of three systems. The enough vacuum layer ensured that the models did not interact with their own periodic image in the direction perpendicular to the Au surface.

All calculations were carried out under periodic boundary conditions by fixing the bottom two layers of Au in every system. The cutoff was 9.5 Å for van der Waals (vdW) interactions in the three systems. A atom-based summation with cutoff 9.5 Å was used for Coulomb interactions in the dielectric system (*viz.*, A system) while Ewald summation with accuracy (1 cal/mol) was employed for Coulomb interactions in the B and C systems. After energy minimization using

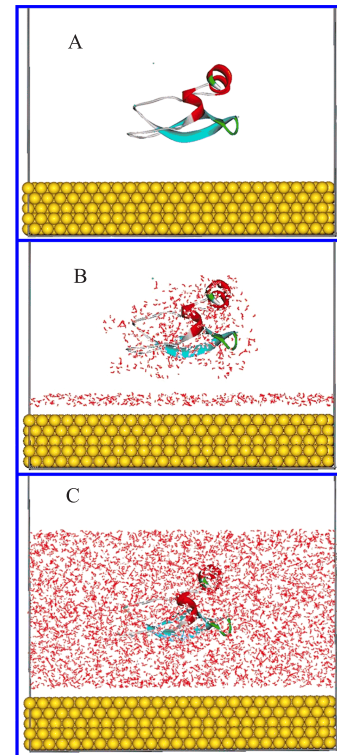


FIG. 1 Three constructed systems A, B, and C are shown. A system, dielectric constant model. B system, partial solvation model with 2.5 Å water layer for the Au(111) surface and the BPTI. C system, full solvation model. The protein is placed in the same orientation and is shown in secondary structure cartoon, the red indicates the  $\alpha$ -helices, the sky-blue represents the  $\beta$ -sheets. Turn in green, coil in grey.

the conjugated gradient method, we carried out a time scale of 10 ns molecular dynamics in the NVT ensemble ( $T=298 \text{ K}$ ). A time step of 2 fs was used in the Velocity Verlet integration. Temperature was controlled by the Anderson thermostat method. The trajectory was saved every 10 ps for analysis. Analysis were performed using tools within the Material Studio and VMD programs [47]. The calculated results showed that the simulations of the three systems achieved stable adsorption states.

## III. RESULTS AND DISCUSSION

### A. Root mean square deviation

Root-mean-square deviation (RMSD) of the BPTI from its crystal structure is calculated and served as an indicator to describe effects of the adsorption on the overall structure of the protein in three water environments. The RMSD value of heavy atoms of the protein is plotted as a function of time in Fig.2 and the calculated average RMSD value over the last 2 ns trajectories is listed in Table I.

TABLE I The average of RMSD<sup>a</sup>,  $R_g$  and three orthogonal components ( $R_g(x)$ ,  $R_g(y)$ ,  $R_g(z)$ )<sup>b</sup>,  $N_{3A}$  and  $N_{5A}$ <sup>c</sup>,  $D_{\text{com-surface}}$ <sup>d</sup> of protein over the final 2 ns trajectories.

System	RMSD/Å	$R_g$ /Å	$R_g(x)$ /Å	$R_g(y)$ /Å	$R_g(z)$ /Å	$D_{\text{com-surface}}$	$N_{5A}$	$N_{3A}$
A	6.948±0.101	13.14±0.09	9.04±0.13	9.06±0.07	2.94±0.10	5.643±0.066	72.8±4.9	246.8±2.4
B	6.054±0.065	11.80±0.07	8.35±0.10	7.50±0.09	3.66±0.06	8.343±0.080	26.6±3.2	82.3±2.2
C	3.861±0.106	11.16±0.07	6.24±0.19	6.48±0.24	6.59±0.20	15.344±0.280	10.3±1.7	30.7±1.3

<sup>a</sup> RMSD value of heavy atoms on the protein is for the deviation from the crystal structure.

<sup>b</sup>  $R_g$  denotes the radius of gyration of the BPTI and  $R_g(x)$ ,  $R_g(y)$ ,  $R_g(z)$  denote the radius of gyration along three orientations, respectively.

<sup>c</sup> The number of non-hydrogen atom within 3 and 5 Å from the Au surface.

<sup>d</sup>  $D_{\text{com-surface}}$  denotes the distance between the mass center of the protein and the Au surface.

Native protein:  $R_g=10.90$  Å,  $R_g(x)=7.33$  Å,  $R_g(y)=6.29$  Å,  $R_g(z)=5.06$  Å.

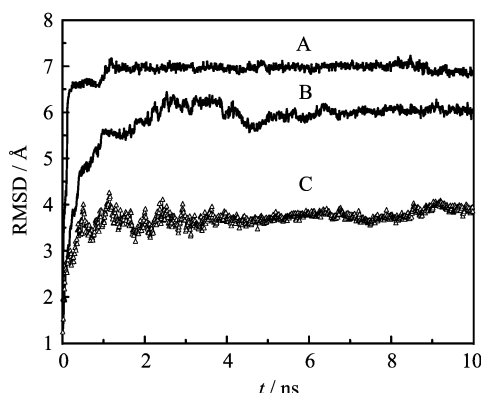


FIG. 2 RMSD values of heavy atoms of BPTI with respect to the simulation time in three systems.

As can be seen from Fig.2, the RMSD of the protein in the A system shows a sharp increase in the initial 150 ps and then rapidly achieves a constant value, while a significant increase in the RMSD value is observed in the B system within the longer time (the first 2 ns), but with less extent. In the following 4 ns, the RMSD changes in the B system experience small fluctuation and gradually approach to equilibration. The observation suggests that the protein in the dielectric environment more easily achieves a stable adsorbed state than that in the partial solvation system. In the C system, the RMSD of protein does not display large increase in initial phase of the adsorption like the A and B systems. Relatively small fluctuation is observed in the initial 4 ns for the C system, after which the RMSD value changes little and almost achieves to be constant. Table I and Fig.2 show that the RMSD value in the three system follows the order of A>B>C. The average RMSD value over the last 2 ns in the B system is smaller by 0.9 Å than that in the A system, implying a role of the water layer in preserving the protein native structure. However, the RMSD values in the A and B systems are higher than 6 Å, suggesting that the structure of the protein in the two models has large deviation from the starting crystal structure. The RMSD value

in the C system is the smallest, almost only half of A system or B system, indicating that an increase in the amount of explicit water could significantly preserve the protein native conformation.

In order to visually view the variation of protein conformation upon adsorption, we selected some representative snapshots on the basis of the RMSD variation to display the adsorption process in the three systems (see Fig.3). As can be seen from Fig.3A, significant conformational changes of the protein is occurred within the first 150 ps in the dielectric model, where the protein rapidly approaches to the Au surface, accompanied with a large spreading along the Au surface. After 150 ps, the overall conformation of the protein does not experience significant changes. Thus, we used the last snapshot to represent the system during the phase between 0.5 and 10 ns time. For the B system, Fig.3B clearly shows a significant conformation variation occurred within the initial 6 ns, exhibiting significant rearrangements of the protein local structure. After 6 ns, no large changes are observed for the overall structure of the protein, as presented by one representative snapshot selected from the last 4 ns simulation trajectories.

For the C system (see Fig.3C), it is clearly observed that there have been no significant conformation variation occurred, different from the A and B systems. Interestingly, it is noted that the protein experiences a rotation to some extent when it approaches to the Au surface before  $t \approx 5$  ns, where the protein tilts itself away the surface and stepwise becomes perpendicular to surface. The observation suggests that enough explicit water molecules could allow the protein to rotate itself for searching an appropriate way to deposit onto surface.

In order to more clearly observe the difference in the protein structure between the three water environments, we superposed the last snapshots of protein in the three systems (see Fig.4). It is apparent that there are significant differences in the final structures of the protein, especially between the C system and the other two. Compared to the C system, the conformations of the protein are relatively similar for the A and B

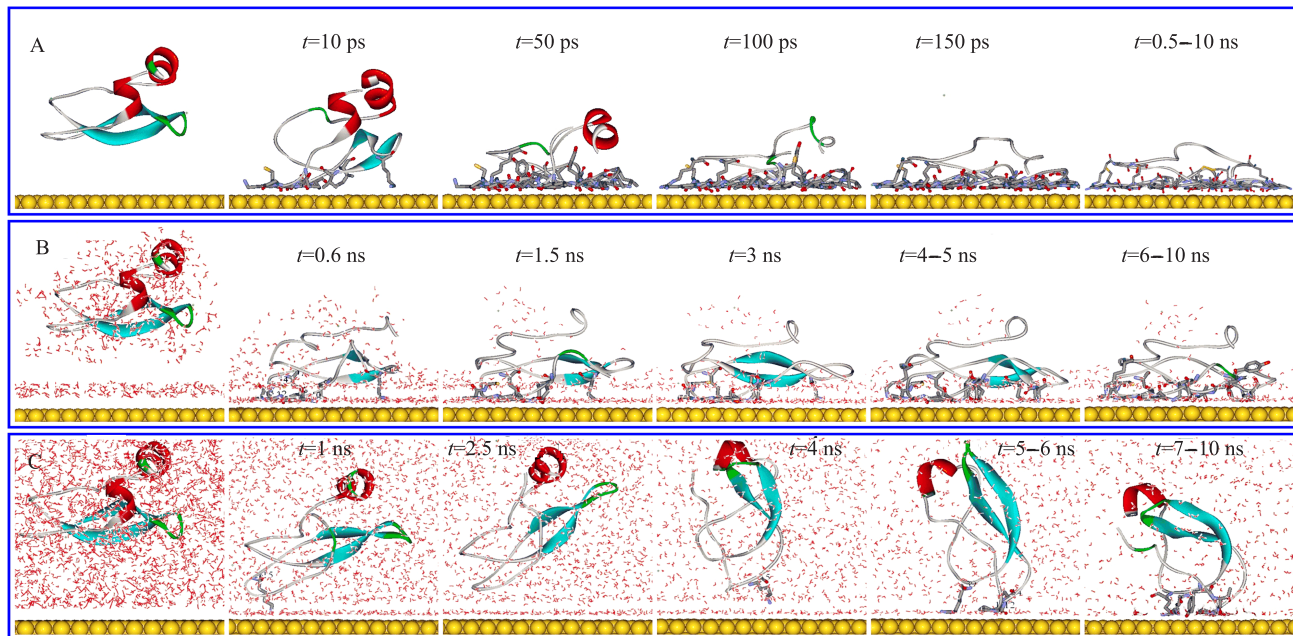


FIG. 3 The representative snapshots of the BPTI protein selected from the 10 ns simulation trajectories on basis of the RMSD variation in the dielectric (A system), partial solvation (B system), and full solvation (C system). All viewed from the front of Au(111) surface. The amino acids within 5 Å of the Au surface are displayed in stick cartoon. the red indicates the  $\alpha$ -helices, the sky-blue represents the  $\beta$ -sheets, turn in green, and coil in grey.

systems, both showing significant spreading parallel to surface, but, also presenting some differences in local structures of the protein.

### B. Radius of gyration

The radius of gyration ( $R_g$ ) is an indicator of compactness of the protein, commonly estimated in terms of Eq.(1) [30],  $N$  is the number of atoms and  $m_i$  and  $r_i$  are the mass and position of atom  $i$ , and  $r_{\text{com}}$  is the center-of-mass position of the protein.

$$R_g = \sqrt{\frac{\sum_{i=1}^N m_i (\mathbf{r}_i - \mathbf{r}_{\text{com}})^2}{\sum_{i=1}^N m_i}} \quad (1)$$

$$R_g(\text{all}) = \sqrt{R_g^2(x) + R_g^2(y) + R_g^2(z)} \quad (2)$$

In addition, the radius of gyration with its three orthogonal components ( $R_g(x)$ ,  $R_g(y)$ ,  $R_g(z)$ ) can best characterize the spreading of protein. Thus, we also calculate the three components using Eq.(1) through replacing the  $r_i$  to  $x_i$ ,  $y_i$ ,  $z_i$ , respectively. Eq.(2) depicts the relationship between the radius of gyration ( $R_g$ ) and its three components ( $R_g(x)$ ,  $R_g(y)$ ,  $R_g(z)$ ). These  $R_g$  values of protein in the three solvent environments are plotted as a function of time in Fig.5. Their

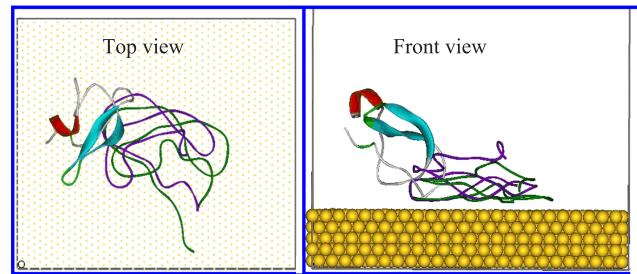


FIG. 4 The superposition of final protein backbone structures in dielectric A system (green), partial solvation B system (purple), full solvation C system (sky-blue). The water molecule is not shown for clarity.

average values calculated over the final 2 ns are listed in Table I. In addition, Table I lists the  $R_g$  and its three orthogonal components of the native protein, calculated using the optimized structure of the crystal structure with restraining on the heavy atoms. An inspection of Table I reveals that the radii of gyration  $R_g$  in the three models follows the order of A>B>C, larger than that of the native protein. The observation suggests that the adsorption makes the protein structure looser, especially in the dielectric model (A system), where the  $R_g$  value is 13.14 and significantly larger than that of the native protein and the other two systems, implying denaturation of the protein occurred.

As can be seen from Fig.5A, in the dielectric model (A system), the perpendicular component  $R_g(z)$  under-

goes a dramatic drop to a very small value in the initial  $\sim 150$  ps while the parallel components ( $R_g(x)$ ,  $R_g(y)$ ) show a sharp increase. After  $\sim 150$  ps, the three values in the A system approach to constant. The observation indicates that the protein is tightly compressed perpendicular to the surface and significantly spreads parallel to the surface within very short time, consistent with the observation from Fig.3, implying a fast and strong adsorption on the Au surface. The variation trend is also consistent with the RMSD and the findings from Raffaini and Ganazzoli [20], who used an effective dielectric constant to study adsorption of Lysozyme onto hydrophobic graphite and also found that the  $R_g(x, y)$  increased dramatically and  $R_g(z)$  decreased clearly. The observations indicate that the fast and strong adsorption of protein can occur on either the hydrophobic surface or the hydrophilic Au surface when the dielectric constant is used to model aqueous solution.

In the B system, a substantial decrease in the  $R_g(z)$  is also observed within longer time (about in the initial 1 ns), but with less extent compared to the A system. Then, a minor decrease in the  $R_g(z)$  has been continued over the following 1 ns time. In the remainder of the simulations, the fluctuation changes small and approaches to an equilibration after  $\sim 6$  ns. The adsorption induced  $R_g(x)$  and  $R_g(y)$  changes do not present sharp increase the same as the A system within initial simulation times, but with significant fluctuations within initial 4 ns in the B system, especially the  $R_g(x)$ . Similarly, the  $R_g(x)$  and  $R_g(y)$  values achieve an equilibration after  $\sim 6$  ns. As can be seen from Table I and Fig.5B, the  $R_g(z)$  value is significantly smaller than the  $R_g(y)$  and  $R_g(x)$  values in the B system, also exhibiting a significant spreading parallel of protein to the surface. Compared to the A system, the  $R_g(z)$  value is larger and the  $R_g(x)$  and  $R_g(y)$  are smaller in the B system, indicating a less spreading extent. The difference in these  $R_g$  values between the A and B systems displays the role of the water layer in influencing the adsorption of the protein.

In the C system, the variations of the  $R_g$  and its three components are significantly different from the A and B systems and exhibit fluctuations with no clear trends (see Fig.5C). For instance, the  $R_g(z)$  displays a rise in initial 4 ns and then small fluctuation in the successive 2 ns and a minor drop between  $t=6$  and 7 ns, afterwards it approaches to constant. While for  $R_g(x)$  value, it stepwise decreases before  $\sim 4$  ns and then displays a minor increase between  $t=4$  and 6 ns, after which it almost keeps constant. Compared to the  $R_g(z)$  and  $R_g(x)$  values, the  $R_g(y)$  does not present a significant variation during the 10 ns simulation, exhibiting minor fluctuation around  $\sim 6.2$  Å. The variation trends of these  $R_g$  values in the C system are inconsistent with the RMSD changes. As revealed above, the RMSD value stepwise increased before  $t=4$  ns and changed little in the rest of simulation. Indeed, the inconsistency was

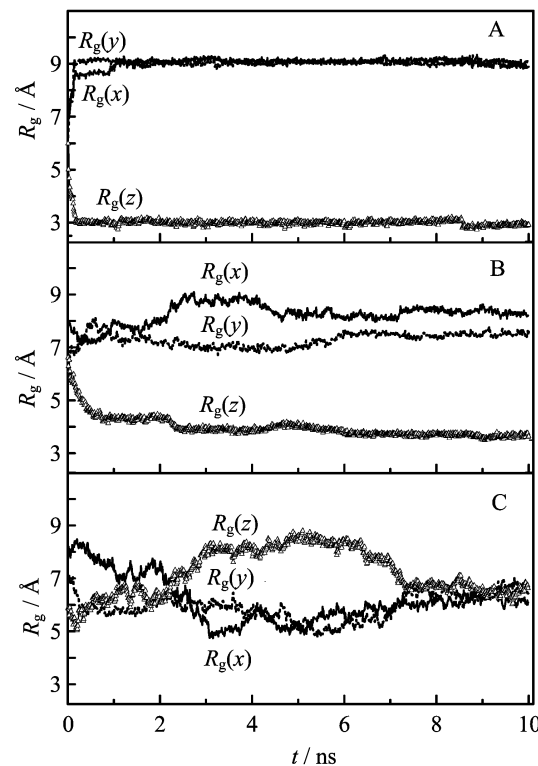


FIG. 5 The time-dependent  $R_g(x)$ ,  $R_g(y)$  and  $R_g(z)$  in the dielectric (A system), partial solvation (B system), and full solvation (C system).

mainly attributed to the rotation behavior of the protein occurred in the initial 5 ns, which leads to a rise of  $R_g(z)$  and a drop of  $R_g(x)$  in the phase. Although the adsorption causes conformation changes of the protein to some extent in the initial phase, the accompanied rotation should weaken the conformation changes, which contributes to the small variation in the RMSD value. Compared to the A and B system, the values of the  $R_g(x)$  and  $R_g(y)$  of the protein are smaller in the C system and the  $R_g(z)$  is larger. Furthermore, the three values in the C system are closer to those of the native structure than the other two systems. The observations suggest that the specific water could to large extent preserve the native conformation of protein and the effect displays to some extent correlation with the amount of explicit water.

### C. Distance between mass center of the protein and Au surface

The distance between the mass center of the protein and the Au surface ( $D_{\text{com-surface}}$ ) is calculated in order to monitor the approaching process of protein toward the Au surface in the three water environments. Figure 6 depicts the variation trend of the distance *vs.* time.

For the A and B systems, the adsorption induced

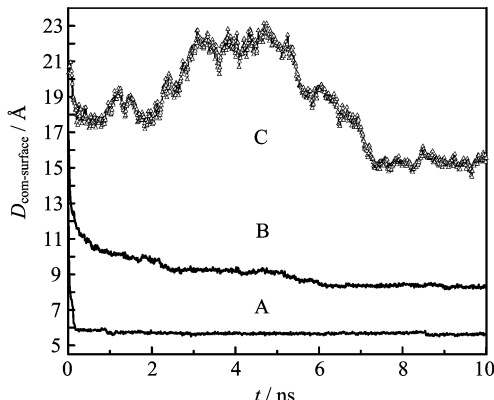


FIG. 6 The distance between center of mass of BPTI and Au surface ( $D_{\text{com-surface}}$ ) as a function of simulation time  $t$  in three systems.

distance changes is consistent with the variations of the RMSD and the radius of gyration. For instance, the distance value in the A system is also sharply decreased within the initial 150 ps and then almost stabilizes at approximately 5.7 Å in the remainder of simulation. While for the B system, the distance significantly decreases within the first 1 ns and then continues to present a slow drop until  $t \approx 6$  ns, after which it achieves constant (about 8.3 Å). In the C system, the  $D_{\text{com-surface}}$  variation also presents fluctuation without a clear trend, similar to the  $R_g(z)$  variation. For example, the distance presents a drop within the first 1 ns, but with much less extent compared to the A and B system. In the following 1 ns, it displays minor fluctuation. Then, the distance is increased from 17.5 Å to 22 Å between  $t=2$  and 3 ns and exhibits to some extent fluctuation around 22 Å between  $t=3$  and 5 ns, afterwards begins to stepwise decrease in the following 2 ns. In the final 3 ns, it almost keeps 15.5 Å. Similarly, the abnormal increase between  $t=2$  and 3 ns is also attributed to the rotation of protein occurring within initial 5 ns, as revealed above. The average  $D_{\text{com-surface}}$  values over the final 2 ns in the three systems are in the order of C>B>A (see Table I), also displaying the effects of non-specific and specific solvation on the adsorption and a definite dependence on the extent of specific solvation.

#### D. The secondary structure of protein

To gain more insight into the effect of specific water on the protein conformation variation induced upon adsorption, we calculated the secondary structures of the proteins in the three systems using DSSP algorithm [48, 49]. Herein, we selected 100 snapshots in every system from the 10 ns MD trajectory at interval of 100 ps. Figure 7 shows the number of residues involved in  $\alpha$ -helices and  $\beta$ -sheets in the 100 frames and Fig.8 further displays types of these residues involved in the secondary

TABLE II The secondary structure of native protein-BPTI.

Name and serial number of amino acid	
$\alpha$ -helix	
1st	Asp3-Phe4-Cys5-Leu6
2nd	Ala48-Glu49-Asp50-Cys51-Met52-Arg53-Thr54-Cys55
$\beta$ -sheet	
1st	Ile18-Ile19-Arg20-Tyr21-Phe22-Tyr23-Asn24
2nd	Leu29-Cys30-Gln31-Thr32-Phe33-Val34-Tyr35

structure.

Figure 7 clearly shows that no  $\alpha$ -helices is observed for the 100 snapshots in the A system while the  $\beta$ -sheets occasionally appear only in 5 frames of the 100 snapshots, suggesting that the protein completely loses its secondary structure and does undergo dramatic structure changes owing to the fast and strong adsorption in the dielectric model. Figure 8 further reveals that there are only several residues participating in the parallel  $\beta$ -sheets in the five snapshots, which are not native  $\beta$ -sheet residues listed in Table II. Raffaini and Ganazzoli used MD simulation with an implicit water solvent to study the adsorption of human lysozyme on hydrophobic graphite and also observed that no secondary structure was present in the final stable state [20]. Combined with our findings, it can be drawn that the dielectric model results in a fast disappearance of all secondary structure of protein induced upon adsorption on either hydrophilic or hydrophobic surfaces.

Similar to the A system, there is nearly no  $\alpha$ -helices presented in the 100 snapshots for the B system, with the exception of one frame. But, the  $\beta$ -sheets have existed over the initial 6 ns, as reflected by Fig.7B. However, the protein finally loses its all  $\beta$ -sheets in the rest of the MD simulation. An inspection of Fig.8 and Table II further reveals that the initial residues involved in the  $\beta$ -sheets of the native protein are mostly preserved before  $t=6$  ns, accompanied some other amino acids (for example, serial number of 49 and 50 amino acids) occasionally joining in the  $\beta$ -sheets. These observations imply that the protein also experiences to some extent denaturation in the B system despite the existence of 2.5 Å water layer, which cannot prevent the final disappearance of all secondary structure.

Different from the A and B systems, the  $\alpha$ -helices and  $\beta$ -sheets have almost existed in the C system over the whole simulation time, although the number of residues involved in the second structure displays to some extent fluctuation upon adsorption, as shown in Fig.7. A comparison of Fig.8 with Table II further reveals that the first  $\alpha$ -helix presented in the native protein while the second  $\alpha$ -helix has been almost preserved. The two  $\alpha$ -helices are located at upside of the protein along the  $z$  direction from the Au surface and the first  $\alpha$ -helix is closer to the surface than the second one, as shown in

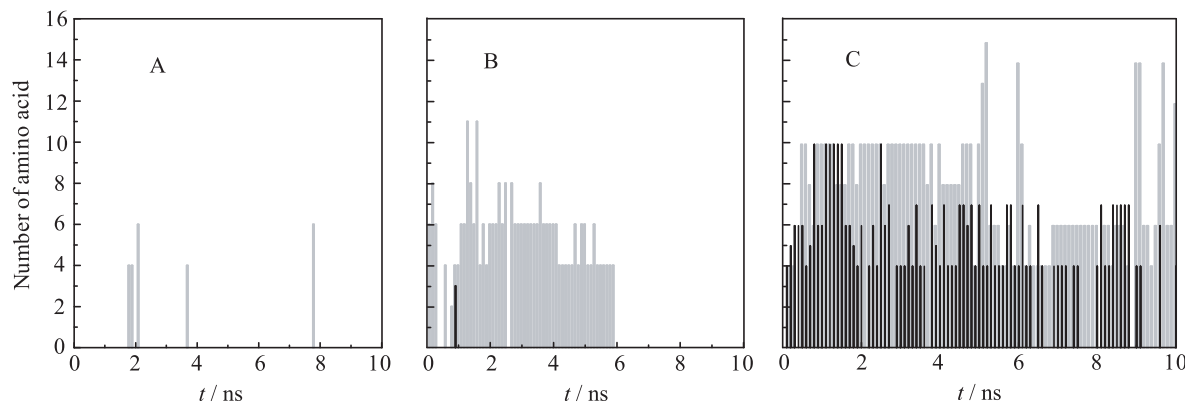


FIG. 7 The number of amino acids involved in  $\alpha$ -helices or  $\beta$ -sheets calculated using DSSP algorithm for the 100 snapshots selected from the 10 ns trajectories at 100 ps interval in A system, B system, and C system. The black and grey lines denote  $\alpha$ -helices and  $\beta$ -sheets, respectively.

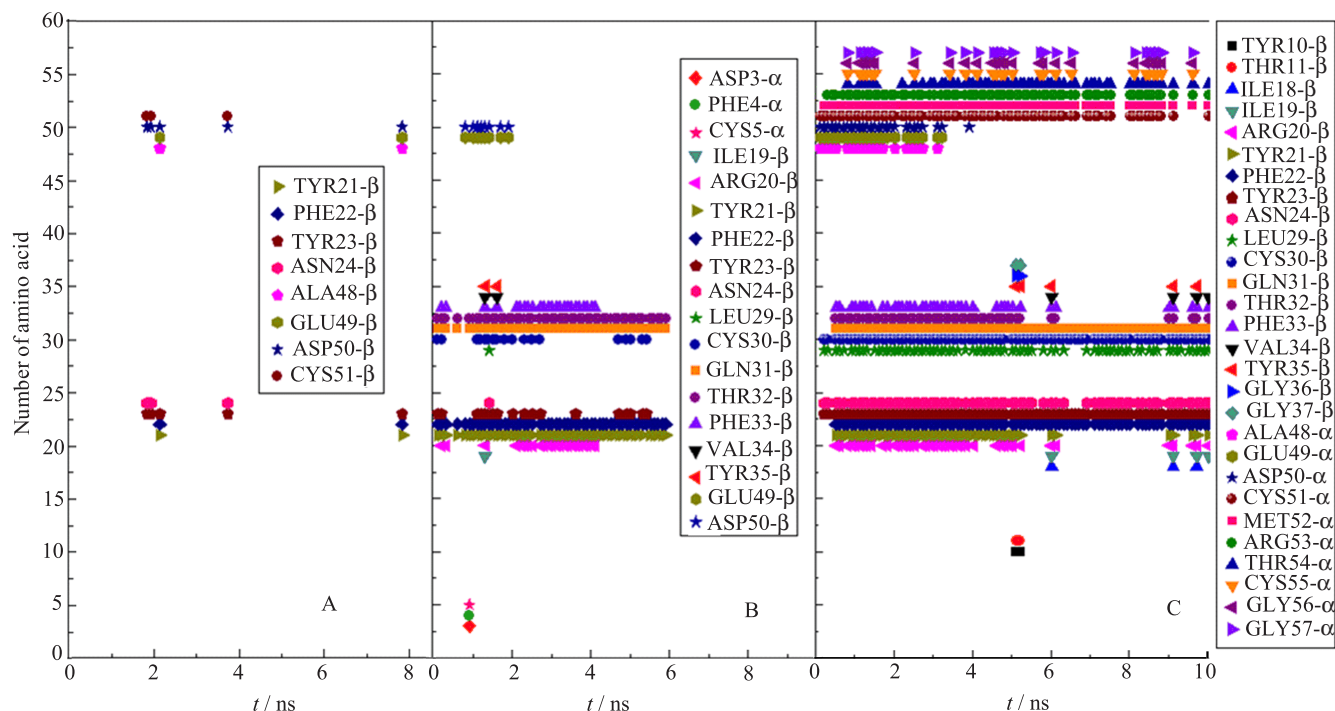


FIG. 8 The type of amino acids involved in the secondary structure, derived from the 100 frames in A system, B system, and C system. In every system, the 100 frames are selected per 100 ps of 10 ns simulation trajectories.

Fig.1. Similarly, some amino acids not involved in the native  $\beta$ -sheets (for example, the serial number: 10, 11, 36, 37) also participate in the  $\beta$ -sheet structures during simulation time while some native  $\beta$ -sheet residues are remained in the structure, exhibiting some rearrangements in the local structure of the protein. The observations indicate that the enough and explicit water molecule can render the protein to preserve its native structure to large extent. As a result, the RMSD of the protein in the C system is significantly smaller than those in the A and B systems.

### E. Adsorbed atoms

In order to quantify the extent of protein adsorption on the Au surface, we calculated the number of adsorbed non-hydrogen atoms within 3 Å ( $N_{3A}$ ) and 5 Å ( $N_{5A}$ ) distances from the surface, which are generally served as criterions of direct (or strong) and indirect (or weak) contact with the gold surface, respectively [27, 30, 33, 50]. The calculated results are listed in Table I and shown in Fig.9.

As shown in Fig.9, the number of adsorbed atoms in the A system is sharply increased to  $\sim 225$  and  $\sim 70$

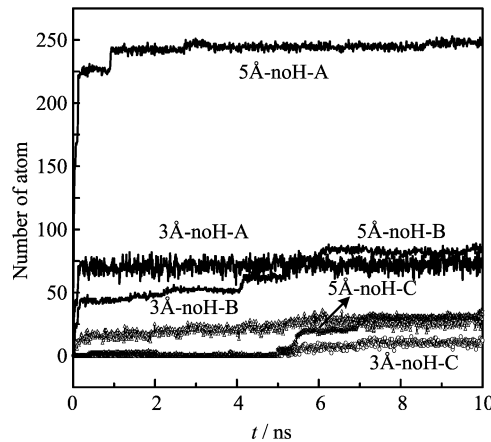


FIG. 9 The number of non-hydrogen atoms less than 3 Å (labeled as 3Å-noH) and 5 Å (labeled as 5Å-noH) from the surface along  $z$  axis in dielectric (A system), partial solvation (B system), and full solvation (C system) environments with respect to time.

for the  $\leq 5$  Å and  $\leq 3$  Å distances from the surface within initial 150 ps, respectively. The average number of atoms adsorbed over the last 2 ns trajectory is calculated to be 247 and 73 for the 5 and 3 Å distances, respectively, which corresponds to 56% and 16% fraction of total non-hydrogen atoms of protein, respectively. The observation further confirms that a strong adsorption is occurred within very short time in the dielectric model, which in turn leads to large conformation changes of the protein, as demonstrated by the RMSD value, the  $R_g$  value, and the secondary structures above.

For the B system, the adsorption induces a few atoms of the protein to enter into the 5 and 3 Å regions within several hundred ps. The number of adsorbed atoms has been stepwise increased to be  $\sim 82$  for 5 Å (about 18% fraction of the protein) and  $\sim 27$  for 3 Å (equal to be 6% fraction adsorbed) in the following  $\sim 6$  ns time and then almost achieves constant. Compared to the A system, the number of adsorbed atoms over the last 2 ns is much smaller (82 vs. 247 for 5 Å and 27 vs. 73 for 3 Å), which contributes to less conformation changes induced upon adsorption in the B system, as confirmed by smaller RMSD and  $R_g$  values above. As can be seen from Fig.3, there are water molecules located between the protein and the surface, which play a significant role in hindering larger number of atoms to interact with the surface, accordingly, rendering the smaller conformation variation of the protein.

In the C system, no atoms of protein are adsorbed into the 3 Å region within initial 5 ns time while few atoms are occasionally adsorbed into the 5 Å region, as shown in Fig.9. But, the adsorption in the phase still results in observable changes in the protein structure, as revealed by the RMSD and  $R_g$  above. After 5 ns, some atoms begin to be adsorbed into the 5 and 3 Å region

and the number of atoms adsorbed is slowly increased in the following  $\sim 2$  ns, and remains to be about 10 and 31 atoms for the 3 and 5 Å regions in the final 3 ns simulation, respectively, smaller than the half of those in the B system. A drop of  $D_{\text{com-surface}}$  between  $t=5$  and 7 ns in the C system reveals that the adsorbed atoms over the phase still induce the protein to approach to the surface. But, the adsorption in the phase only causes minor conformation changes in the overall structure of the protein since the RMSD and  $R_g$  values only exhibit small fluctuations. In the phase  $t=5$  and 7 ns, there are mainly some minor rearrangements, judged from the RMSD and the secondary structure variations above. In addition, we also notes that there is not large difference in the RMSD of protein between the A and B systems, both much higher than that in the C system, although the adsorbed atoms in the B system are much smaller than that in the A system owing to the expulsive effect of water layers located between the protein and the surface in the B system. It seems a bit abnormal since the number of adsorbed atoms in the B system is relatively close to that in the C system with similar expulsive effects derived from the water layer. But, why is the RMSD in the B system much higher than the C system and is close to the A system with much more atoms adsorbed? To address this question, we examined the conformation variations upon the adsorption and found that the initial water molecules around the protein in the B system are to large extent stripped off during the simulation time and approach to the surface due to the adsorption, as revealed by Fig.3.

However, the behavior cannot occur in the fully solvated system with explicit water (the C system). Thus, it is reasonable to assume that the adsorption induced escape of some explicit water from the protein (especially the bound water molecules) should contribute to the large conformation changes in the B system. In order to examine the assumption, the protein without any specific water molecules and the Au surface was simulated in the dielectric model, using 10 ns MD simulation. The RMSD value of the isolated protein over the last 2 ns trajectory is observed to high up to be 5.38 Å, only smaller by 0.7 Å than the B system. The observation suggests that there are still high RMSD in the dielectric model despite absence of the surface adsorption, revealing that the large conformation variation of the protein in the B system to large extent stem from the lack of water molecules bound to the protein. The result provides a support for the assumption above, further confirming the role of explicit water bound to protein in preserving the protein native structure and weakening the effect of the adsorption.

#### IV. CONCLUSION

In the work, we used MD simulation to study the adsorption of BPTI on the Au(111) surface in the three types of water environments (dielectric constant, par-

tial solvation, and full solvation), with an objective to explore the roles of non-specific and specific solvation as well as the extent of specific solvation in influencing the structure of protein and the adsorption behavior.

The result shows that the protein presents a fast and strong adsorption within very short time in the dielectric model, which leads to the nearest distance between the protein and the surface and the most number of atoms in contact with the surface in the three systems. Accordingly, the large conformation variation is observed in the dielectric model, as revealed by the highest RMSD, the largest radius of gyration  $R_g$ , largely spreading to the surface and the quick disappearance of all secondary structure. The partial solvation renders some explicit water molecules to interact with the protein and locate near the surface, which to some extent weakens the effect of adsorption. Thus, it exhibits slower adsorption and less changes in the calculated properties above with respect to the dielectric model. However, the significant decrease in the hydration of the protein induced upon the adsorption of polar Au surface, still results in large structure changes in the partial solvation environment similar to the dielectric one (for example, high RMSD and final disappearance of all secondary structure), despite its much less adsorption extent and a slower absorption dynamic than dielectric model. The observation clearly shows the importance of some bound water to protein in the adsorption. Enough water molecules in the full solvation system most preserve the protein native structure through effectively hydrating the protein and the surface, which to larger extent weakens the adsorption effect compared to the partial solvation. As a result, the slowest and weakest adsorptions are observed for it, including the smallest deviation from the native protein and most preservation of secondary structure and much less number of atoms interacted with the surface. In addition, the enough water molecules could allow the protein to rotate to some extent to search a appreciate position to deposit on the surface. The behavior could not occur in the dielectric and partial solvation environments, showing the importance of hydration extent in the adsorption.

On a whole, the effects of non-specific and specific solvation on the protein structure and adsorption behavior are significantly different and the water molecules bound to the protein should play an important role in preserving protein native structure. These observations clearly highlight the importance of the specific interaction of protein-water-surface for the protein adsorption on Au surface, also suggesting that the simulations using implicit water should be treated and interpreted with great care.

## V. ACKNOWLEDGMENTS

This work was supported by the National Natural Science Foundation of China (No.21273154, No.U1230121,

and No.21125313), the Science & Technology Department of Sichuan Province (No.2011H0003 and No.2011HH0005), and the Ministry of Education of China (No.NCET-11-0359 and No.2011SCU04B31). The computation resource in Shanghai Supercomputer Center is also acknowledged.

- [1] M. Calvaresi, S. Hoefinger, and F. Zerbetto, *Chem. Eur. J.* **18**, 4308 (2012).
- [2] X. Dong, Q. Wang, T. Wu, and H. Pan, *Biophys. J.* **93**, 750 (2007).
- [3] V. Hlady and J. Buijs, *Curr. Opin. Biotechnol.* **7**, 72 (1996).
- [4] Q. Chen, Q. Wang, Y. C. Liu, T. Wu, Y. Kang, J. D. Moore, and K. E. Gubbins, *J. Chem. Phys.* **131**, 015101 (2009).
- [5] M. A. Cole, N. H. Voelcker, H. Thissen, and H. J. Griesser, *Biomaterials* **30**, 1827 (2009).
- [6] S. Brown, *Nat. Biotechnol.* **15**, 269 (1997).
- [7] H. Chen, L. Yuan, W. Song, Z. Wu, and D. Li, *Prog. Polym. Sci.* **33**, 1059 (2008).
- [8] F. Hook, B. Kasemo, M. Grunze, and S. Zauscher, *ACS Nano* **2**, 2428 (2008).
- [9] R. A. Petros and J. M. DeSimone, *Nat. Rev. Drug Discov.* **9**, 615 (2010).
- [10] P. Thevenot, W. Hu, and L. Tang, *Curr. Top. Med. Chem.* **8**, 270 (2008).
- [11] L. D. Li, H. T. Zhao, Z. B. Chen, X. J. Mu, and L. Guo, *Biosens Bioelectron.* **30**, 261 (2011).
- [12] M. Rabe, D. Verdes, and S. Seeger, *Colloid Interface Sci.* **162**, 87 (2011).
- [13] A. Vallee, V. Humblot, and C. M. Pradier, *Acc. Chem. Res.* **43**, 1297 (2010).
- [14] J. J. Gray, *Curr. Opin. Struc. Biol.* **14**, 110 (2004).
- [15] Y. C. Lin, Z. X. Cao, and Y. R. Mo, *J. Am. Chem. Soc.* **128**, 10876 (2006).
- [16] R. B. Wu, H. J. Xie, Z. X. Cao, and Y. R. Mo, *J. Am. Chem. Soc.* **130**, 7022 (2008).
- [17] L. T. Da, D. Wang, and X. H. Huang, *J. Am. Chem. Soc.* **134**, 2399 (2012).
- [18] M. J. Yang, X. Q. Pang, X. Zhang, and K. L. Han, *J. Struct. Biol.* **173**, 57 (2011).
- [19] G. Raffaini and F. Ganazzoli, *Langmuir* **19**, 3403 (2003).
- [20] G. Raffaini and F. Ganazzoli, *Langmuir* **26**, 5679 (2010).
- [21] C. Muecksch and H. M. Urbassek, *Langmuir* **27**, 12938 (2011).
- [22] C. Muecksch and H. M. Urbassek, *Chem. Phys. Lett.* **510**, 252 (2011).
- [23] K. Kubiak and P. A. Mulheran, *J. Phys. Chem. B* **113**, 12189 (2009).
- [24] K. Kubiak and P. A. Mulheran, *Langmuir* **26**, 15954 (2010).
- [25] K. Kubiak and P. A. Mulheran, *J. Phys. Chem. B* **115**, 8891 (2011).
- [26] C. Y. Wu, M. J. Chen, and C. Xing, *Langmuir* **26**, 15972 (2010).
- [27] T. Utesch, G. Daminelli, and M. A. Mroginski, *Langmuir* **27**, 13144 (2011).

- [28] G. Raffaini and F. Ganazzoli, *Philos. Trans. Roy. Soc. A* **370**, 1444 (2012).
- [29] A. N. Cormack, R. J. Lewis, and A. H. Goldstein, *J. Phys. Chem. B* **108**, 20408 (2004).
- [30] A. V. Verde, J. M. Acres, and J. K. Maranas, *Biomacromolecules* **10**, 2118 (2009).
- [31] M. Hoefling, F. Iori, S. Corni, and K. E. Gottschalk, *Langmuir* **26**, 8347 (2010).
- [32] A. V. Verde, P. J. Beltramo, and J. K. Maranas, *Langmuir* **27**, 5918 (2011).
- [33] H. Heinz, B. L. Farmer, R. B. Pandey, J. M. Slocik, S. S. Patnaik, R. Pachter, and R. R. Naik, *J. Am. Chem. Soc.* **131**, 9704 (2009).
- [34] R. Artali, A. D. Pra, E. Foresti, I. G. Lesci, N. Roveri, and P. Sabatino, *J. R. Soc. Interface* **5**, 273 (2008).
- [35] J. W. Shen, T. Wu, Q. Wang, and H. H. Pan, *Biomaterials* **29**, 513 (2008).
- [36] A. Calzolari, G. Cicero, C. Cavazzoni, R. D. Felice, A. Catellani, and S. Corni, *J. Am. Chem. Soc.* **132**, 4790 (2010).
- [37] A. F. Oliveira, S. Gemming, and G. Seifert, *J. Phys. Chem. B* **115**, 1122 (2011).
- [38] A. F. Oliveira, S. Gemming, and G. Seifert, *Materialwiss. Werkstofftech.* **41**, 1048 (2010).
- [39] G. Reddy and A. Yethiraj, *Macromolecules* **39**, 8536 (2006).
- [40] G. Reddy and A. Yethiraj, *J. Chem. Phys.* **132**, 074903 (2010).
- [41] E. N. Baker and R. E. Hubbard, *Prog. Biophys. Mol. Bio.* **44**, 97 (1984).
- [42] T. Blundell, D. Barlow, N. Borkakoti, and J. Thornton, *Nature* **306**, 281 (1983).
- [43] N. M. Micaelo and C. M. Soares, *Febs. J.* **274**, 2424 (2007).
- [44] H. Heinz, R. A. Vaia, B. L. Farmer, and R. R. Naik, *J. Phys. Chem. C* **112**, 17281 (2008).
- [45] W. L. Jorgensen, J. Chandrasekhar, J. D. Madura, R. W. Impey, and M. L. Klein, *J. Chem. Phys.* **79**, 926 (1983).
- [46] L. J. Zhu, W. Yang, Y. Y. Meng, X. C. Xiao, Y. Z. Guo, X. M. Pu, and M. L. Li, *J. Phys. Chem. B* **116**, 3292 (2012).
- [47] W. Humphrey, A. Dalke, and K. Schulten, *J. Mol. Graph. Model.* **14**, 33 (1996).
- [48] W. Kabsch and C. Sander, *Biopolymers* **22**, 2577 (1983).
- [49] R. D. King and M. J. E. Sternberg, *Protein Sci.* **5**, 2298 (1996).
- [50] X. Yu, Q. M. Wang, Y. N. Lin, J. Zhao, C. Zhao, and J. Zheng, *Langmuir* **28**, 6595 (2012).